A Preliminary Thermal-hydraulics Analysis for the NIST Neutron Source

Idan R. Baroukh *†, Anil Gurgen*‡, Joy S. Shen*, Abdullah G. Weiss*

**NIST Center for Neutron Research, 100 Bureau Drive, Gaithersburg, MD 20899, USA*
† NRCN Nuclear Research Center of the Negev, Israel
‡ Department of Materials Science and Engineering, University of Maryland, College Park, MD 20742, USA
idan.baroukh@nist.gov; *anil.gurgen@nist.gov; joy.shen@nist.gov; abdullah.weiss@nist.gov*

doi.org/10.13182/T127-39559

INTRODUCTION

The existing reactor at the NIST Center for Neutron Research (NCNR), the National Bureau of Standards Reactor (NBSR) is a 20 MW D_2O-moderated and reflected tank-type research reactor that has been in operation since 1967. Throughout its tenure, it has served as a vital neutron source for the scientific community, with cold neutron testing capabilities. With the increasing demand for experiments made possible by the NBSR (nearly doubling over the last five years) and the aging of the NBSR with recently longer-lasting outages and increased maintenance expenditures, a replacement reactor is sought-after.

An investigation for a replacement reactor, or the NIST Neutron Source (NNS), are ongoing at the NCNR where pre-conceptual design research is currently pursued. One such activity is a preliminary analysis that attempts to understand the thermal-hydraulics behavior of the NNS design. This paper summarizes these preliminary efforts, which include the development of a low-order thermal-hydraulics model for the entire core. Analyses discussed in this paper include the pressure drop across the core, bulk temperature distributions, and power peaking factors.

METHODOLOGY

This work utilizes a custom-developed computational tool that includes thermal and hydraulics models that can be coupled or decoupled to investigate different physical phenomena throughout the NNS core. This section explains the different models implemented and describes the core geometry and how it is discretized in the models. Solution methodology for the coupled model is also discussed.

Geometry

The NNS core consists of nine fuel assemblies (FA) that are arranged in a 3x3 array. Each FA contains 21 fuel elements (FEs) which are each curved for structural stability. There are six control blades placed in two guide boxes. The guide boxes divide the core horizontally into three rows; therefore, there are 64 coolant channels at each row. The top view of the reactor core is given in Fig. 1. Each FA is fitted to a leg that provides additional stability and generates a bypass flow through a rectangular opening.

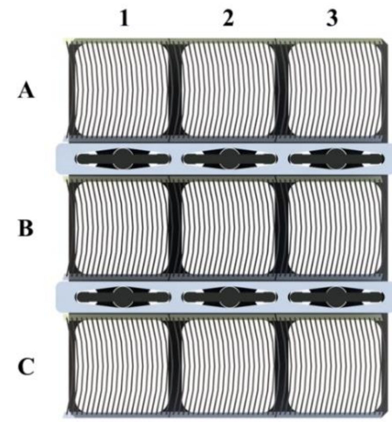

Fig. 1. A top view of the reactor core.

The legs are better viewed when looking at a section view on the side of the core, as shown in Fig. 2. This view lends itself nicely to setting up a simplified diagram of the flow through the core, where the flows through the FAs are clearly bounded by the entrance (bottom) and outlet (top) of the core. Note that this view neglects the presence of the fuel plates, which is acceptable for this pre-conceptual analysis.

Fig. 2 A side view of the reactor core.

Thermal Model

The thermal model calculates the single-phase convective heat transfer between the fuel elements and the coolant. The power for each fuel element is calculated beforehand using the peaking factors from a separate neutronics analysis. The wall heat flux profile is then used to calculate bulk coolant temperature and cladding wall temperature. In order to compute the heat transfer coefficient, Petukhov and Kirillov correlation [1] is used. The basic assumptions of the thermal model are as follows.

- The coolant channel is approximated with a rectangular channel, at which the channel gap is constant, and the coolant velocity is the average velocity at the cross section.
- The generated heat dissipates symmetrically from each side of the fuel element.
- The power density is uniform within a fuel cell element.
- The specific heat at each cell is evaluated at the inlet temperature of the cell.

Hydraulics Model

The hydraulics model calculates the flow distribution and pressure drop across the FAs. The model simulates parallel coolant channels that are connected to a shared inlet and shared outlet plenum, which means that the pressure drop across any given channel is the same. The diagram of a single row with three FAs are given in Fig. 3. It can be seen from the diagram that there are 4 different channel types in the hydraulics model. Due to curved nature of the FE, the coolant channel between chimney and the first FA, is not equal to the last FA and chimney. All the associated coolant channels are calculated considering the geometry specifications of the core.

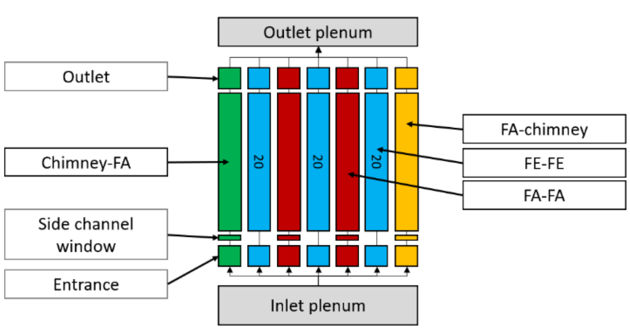

Fig. 3. Diagram of FAs in a single row of the core.

The hydraulics model uses pressure drop equation which is the integrated version of the 1-D momentum equation. For each coolant channel, the model computes the total friction pressure drop and local pressure drop at entrance and exit of each channel as a function of cell average velocity and temperature. In order to calculate friction factor, the Churchill correlation [2, 3] is used.

Coupled Thermal-hydraulics Full-core Model

Coupling the thermal and hydraulics models yields a consolidated model that solves for the reactor's thermal-hydraulics characteristics iteratively. In each iteration the thermal model calculates the bulk coolant temperature and cladding temperature for a given mass flow rate. Then the hydraulics model computes the pressure drop for the calculated temperatures and yields the mass flow rate distribution across all channels. The iterations are continued until the inlet and outlet mass flow rates are converge to the pre-defined input value (Table I). The calculation scheme is illustrated in Fig. 4.

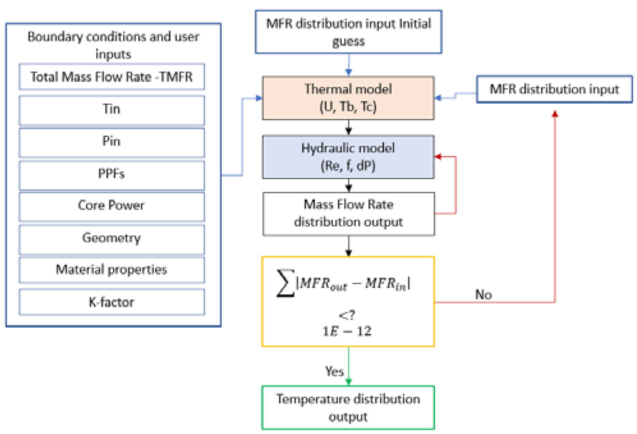

Fig. 4. The computation scheme for the coupled thermal-hydraulics model.

RESULTS & DISCUSSION

This section summarizes the full-core calculation. The boundary conditions and user inputs are given in Table I. The coupled thermal-hydraulics model is tested for accuracy and stability before the full-core calculation. The thermal model is validated by testing the energy balance at a uniform power density. This includes comparing the power input with the total core power and testing the thermal model correlation applicability. For the verification of the hydraulics model, mass flow rate distribution is calculated numerically with different initial guesses. It is observed that the solution converges to the same mass flow rate distribution for each different initial guess.

Table I. Boundary conditions and user inputs

Parameter	Value	Units
Core thermal power	20	MW
Total mass flow rate	540	kg/s
Bypass percentage	10	%
Coolant inlet temperature	316.5	K
Side channel window K factor	0.5	–
Inlet K factor	0.5	–
Outlet K factor	1.0	–
Pressure convergence rate	10^{-13}	MPa
Mass flow rate convergence criteria	10^{-12}	kg/s
Friction correlation	Churchill [2, 3]	–
Nusselt number correlation	Petukhov & Kirillov [1]	–
Power density distribution	MCNP Model	–
Power peaking factor	MCNP Model	–

The calculations are done for 4 different core states, start-up (SU), beginning of cycle (BOC), middle of cycle (MOC), and end of cycle (EOC). The power density distribution and power peaking factors are calculated with a separate neutronics model in the MCNP code [4,5]. In each reported plot, FEs are marked from left to right with a number increasing from 1-63, and the coolant channels are marked from 1-64 from left to right (relative to Fig. 1). The FA rows are marked from top to bottom, by A, B, and C respectively.

The mass flow rate and outlet temperature distributions are shown for SU in Fig. 5 and Fig. 6, respectively, and the results of all other states are summarized in the tables. The mass flow rate distribution follows a nearly uniform distribution at the channels between FEs, indicating that the mass flow rate is not strongly correlated to the power peaking factors. The mass flow rate distribution is affected by the power peaking factors (power) distribution; however, the effects are not significant. Additionally, mass flow rates at channels between FA-FA and FA-chimney are higher than mass flow rate at coolant channels between FEs, because the flow areas at these channels are higher. Similar behavior is observed for BOC, MOC, and EOC.

Table II. Hottest channel coolant temperature comparison

Core State	Max $T_{coolant}$ (K)	Channel	Row
SU	332.5	2	C
BOC	332.4	2	A
MOC	332.9	63	B
EOC	329.8	63	B

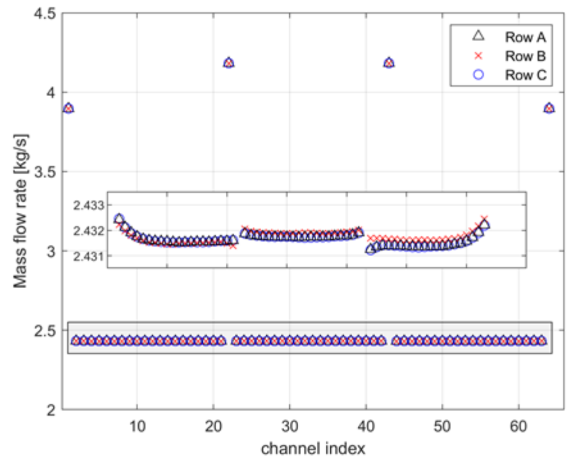

Fig. 5. The mass flow rate distribution at SU.

The coolant temperature is strongly influenced by the power and mass flow rates in the FEs. For the given power density distribution and the calculated mass flow rate distribution, the outlet coolant temperatures of each channel are given in Fig. 6. For different core states, the maximum coolant temperatures are given in Table II. The hottest temperatures are reached at SU and BOC, which is due to the excess reactivity in the core.

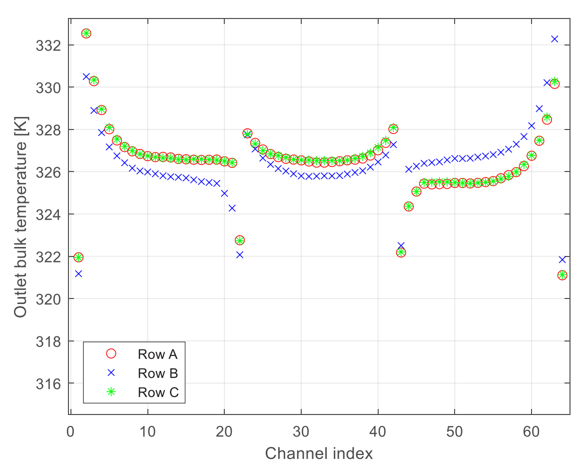

Fig. 6. The outlet coolant temperatures at SU.

Cladding temperature distributions of row C at SU is given in Fig. 7. The plot shows the axial cladding temperature distribution for the first (1), last (63), and some intermediate FEs in row C including those at the interface of each two FAs. For SU, the highest cladding temperature is observed to be 360.9 K at the first FE at row C. Rows A and B have very similar distributions across their FEs.

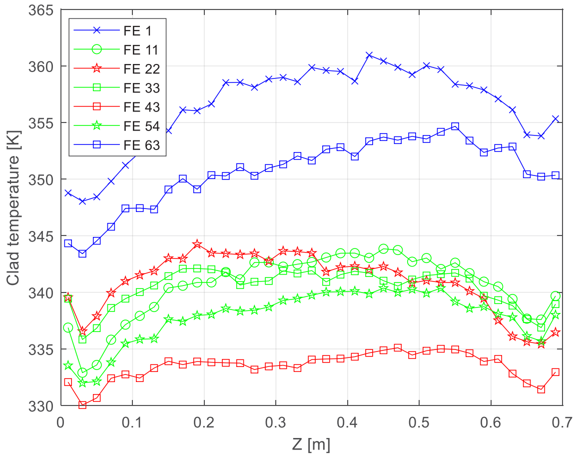

Fig. 7. The axial temperature distributions of clad walls in row C at SU.

For other core states, the maximum cladding temperatures and their corresponding FEs are given in Table III. Note that these temperatures reflect the "wall" temperatures of the clad and are closer to being the film temperatures at the wall than the actual temperature of the clad. Accounting for the clad temperature requires modeling conduction effects, which is currently being pursued.

Table III. The hottest clad wall temperature at each core state.

Core State	Max T_{clad} (K)	FE	Row
SU	360.9	1	C
BOC	360.5	1	A
MOC	358.4	63	B
EOC	355.0	63	B

The thermal limits for different core states are given in Table IV, where the critical heat flux needed to compute minimum departure from nucleate boiling ratio (mDNBR) is obtained using the Sudo-Kaminaga correlation [6]. The onset of flow instability ratio (OFIR) is computed using the Saha-Zuber correlation [7]. Across all core states, the core maintains a relatively stable mDNBR and OFIR, where it increases as the core proceeds through its cycle. The mDNBR is always greater than 2, which agrees with the general guidance provided in NUREG 1537 [8], but it barely passes 2, and as such, additional core optimization is likely needed in future reactor design activities.

Table IV. The thermal limits at different core states.

Core State	mDNBR	OFIR
SU	2.22	12.9
BOC	2.18	13.6
MOC	2.42	15.2
EOC	2.61	15.1

CONCLUSIONS

A custom single phase thermal-hydraulics analysis code was developed to perform analyses on the NNS. The code coupled separate thermal and hydraulics 1D models that can perform core-wide system-level computations. A preliminary thermal-hydraulics analysis was conducted to obtain measures of the expected mass flow rates and temperatures in the core. Results show that the channels neighboring a chimney are the hottest because they have significantly higher power at SU and BOC states. This indicates that these channels are likely the most limiting in the core and will dictate future iterations of the design. More detailed investigations are recommended to determine the local pressure losses at those side channels and at the channels' inlet and outlet. A more detailed accounting of the heat flux distribution is also desirable, and conduction effects should also be considered in future iterations of the model.

DISCLAIMER

The identification of certain commercial equipment, instruments, or materials does not imply recommendation or endorsement by the authors or by the National Institute of Standards and Technology. Contributions of NIST are not subject to copyright in the United States.

REFERENCES

1. B.S. PETUKHOV, VV. KIRILLOV, "On the Question of Heat Transfer to a Turbulent Flow of Fluids in Pipes", *Teploenergetika (Thermal Engineering) 4*, 63-68 (1958).
2. S.W. CHURCHILL, "Friction-factor equation spans all fluid-flow regimes", *Chemical Engineering*, **84 (24)**, 91-92 (1977).
3. F. WHITE, *Fluid Mechanics*, p. 371, 7th Ed., McGraw-Hill Series in Mechanical Engineering (2009).
4. C.J. WERNER, "MCNP Users Manual – Code Version 6.2", LA-UR-17-29981, Los Alamos National Laboratory (2017).
5. O.S. CELIKTEN, D. SAHIN, A.G. WEISS, "Highlights of Neutronics Analyses for the Pre-conceptual NIST Neutron Source Design", Trans. Am. Nucl. Soc., 127, (2022).
6. M. Kaminaga, K. Yamamoto, Y. Sudo, "Improvement of Critical Heat Flux Correlation for Research Reactors using Plate-Type Fuel", *Journal of Nuclear Science and Technology*, **35 (12)**, 943-951 (1998).
7. P. Saha, N. Zuber, "Point of net vapor generation and vapor void fraction in subcooled boiling", *Proceedings of the 5th International Heat Transfer Conference*, **4** (1974).
8. NUREG-1537, "Guidelines for Preparing and Reviewing Applications for the Licensing of Non-Power Reactors", *U.S. Nuclear Regulatory Commission* (1996).